

Organic & Biomolecular Chemistry

Accepted Manuscript

This article can be cited before page numbers have been issued, to do this please use: T. Shi, S. Teng, G. K. R. Alavala, X. Guo, Y. Zhang, K. T. Moore, T. Buckley, D. Mason, W. Wang, E. Chapman and W. Hu, *Org. Biomol. Chem.*, 2019, DOI: 10.1039/C9OB01903K.



This is an Accepted Manuscript, which has been through the Royal Society of Chemistry peer review process and has been accepted for publication.

Accepted Manuscripts are published online shortly after acceptance, before technical editing, formatting and proof reading. Using this free service, authors can make their results available to the community, in citable form, before we publish the edited article. We will replace this Accepted Manuscript with the edited and formatted Advance Article as soon as it is available.

You can find more information about Accepted Manuscripts in the [Information for Authors](#).

Please note that technical editing may introduce minor changes to the text and/or graphics, which may alter content. The journal's standard [Terms & Conditions](#) and the [Ethical guidelines](#) still apply. In no event shall the Royal Society of Chemistry be held responsible for any errors or omissions in this Accepted Manuscript or any consequences arising from the use of any information it contains.

ARTICLE

Catalytic Asymmetric Synthesis of 2,5-Dihydrofurans Using Synergistic Bifunctional Ag Catalysis

Received 00th January 20xx,
Accepted 00th January 20xxTaoda Shi,^{a,b} Shenghan Teng,^a Alavala Gopi Krishna Reddy,^d Xin Guo,^c Yueteng Zhang,^b Kohlson T. Moore,^b Thomas Buckley,^b Damian J. Mason,^b Wei Wang,^b Eli Chapman,^{b*} and Wenhao Hu^{d*}

DOI: 10.1039/x0xx00000x

We report a bifunctional Ag catalyst promoted intramolecular capture of oxonium ylides with alkynes for the enantioselective synthesis of 2,5-dihydrofurans. This represents unprecedented synergistic catalysis of a bifunctional Ag catalyst. Mechanistic studies revealed that [(*R*)-3,5-DM-BINAP](AgSbF₆)₂ (**9**) is likely to be the active catalytic species and that the reaction involves second order kinetics with respect to **9**, suggesting that two molecules of **9** are involved in the intramolecular trapping of a Ag-associated oxonium ylide with a Ag-activated alkyne. Based on our mechanistic hypothesis, we further optimized the reaction, rendering a facile approach to 2,5-dihydrofurans in good to excellent yields in a highly chemo- and enantioselective fashion.

Introduction

In recent years, the development of Ag catalysis in organic synthesis has been well documented.¹⁻⁶ The superior alkynophilicity due to π -coordination with the carbon-carbon triple bond makes Ag salts one of the best activators of alkynes.⁷⁻¹⁰ Despite success in asymmetric Ag catalysis, successful examples of enantioselective Ag-carbenoid transfer (ACT) are rare. The Jørgensen group reported a Ag/BINAP-catalyzed aziridination of iminoesters with trimethylsilyldiazomethane.¹¹ The same group also disclosed a Ag/BOX-catalyzed N-H insertion.¹² The Davies group documented Ag(I)/PHOX-catalyzed cyclopropanation of internal alkynes and donor/acceptor carbenoids.¹³ The Nemoto group recently realized a chiral silver phosphate-catalyzed intramolecular de-aromatization of phenols with excellent enantioselectivities.¹⁴ Motivated by the pioneering work of these researchers, we sought to develop a highly enantioselective ACT via synergistic catalysis of a bifunctional chiral Ag(I)/neutral ligand complex.

The challenges associated with achieving high enantioselectivity in ACT can be attributed to several factors (Scheme 1A-C). First,

enantiocontrol is generally challenging for Ag complexes because the linear or trigonal coordination geometry places the chiral ligand far from the substrate (Scheme 1A).¹⁵ Second, the distance problem is exacerbated if the reaction goes through a Lewis acid pathway where the chiral ligand and the stereogenic center are further separated by two more nitrogen atoms (Scheme 1B).¹² Last, enantioselectivity can be deteriorated by a free carbene pathway even if the ACT proceeds through the carbene pathway (Scheme 1C). It is a formidable task for the Ag-associated carbene to compete against the highly active free carbene for efficient stereoselective control.¹⁶ A successful strategy for a catalytic enantioselective ACT would have to contend with the aforementioned challenges. We hypothesized that two molecules of bifunctional chiral Ag complex could potentially solve these problems, increasing reactivity and enantioselectivity by coordinating the carbene and the alkyne independently (Scheme 1D).

We previously reported a Pd(II)-catalyzed auto-tandem formal [4+1] cycloaddition reaction of aryl diazoacetates and arylpropargyl alcohols to generate 2,5-dihydrofurans, in which the generation of the oxonium ylide and activation of the alkyne were both catalyzed by [PdCl(η^3 -C₃H₅)]₂.¹⁷ We evaluated the biological activities of 2,5-dihydrofurans and identified them as protein tyrosine phosphatase (PTP) inhibitors.^{18, 19} This observation sparked our interest in an asymmetric synthesis of 2,5-dihydrofurans, to determine the relationship between the stereochemistry of 2,5-dihydrofurans and the inhibitory activity against PTPs. In addition to our own biological interests, 2,5-dihydrofurans are an important class of heterocycles that are pharmacophores of FDA approved

^a Shanghai Engineering Research Center of Molecular Therapeutics and New Drug Development, School of Chemistry and Chemical Engineering, East China Normal University, Shanghai, China, 200062.

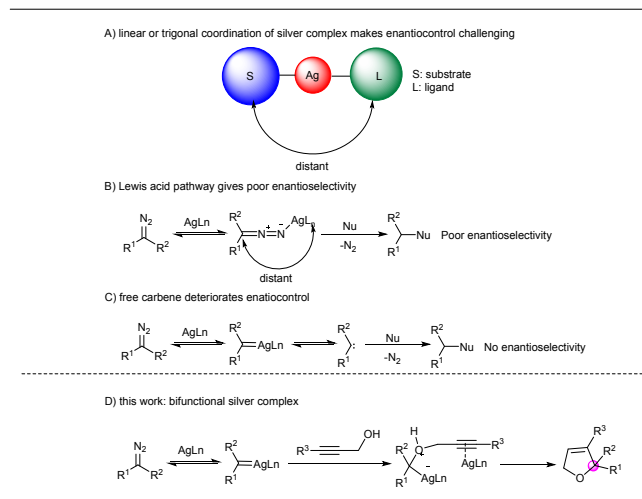
^b College of Pharmacy, Department of Pharmacology and Toxicology, the University of Arizona, Tucson, Arizona 85721.

^c School of Pharmaceutical Sciences, Wenzhou Medical University, Wenzhou, Zhejiang Province, China, 325035.

^d School of Pharmaceutical Sciences, Sun Yat-sen University, Guangzhou, China, 510006.

† Footnotes relating to the title and/or authors should appear here.

Electronic Supplementary Information (ESI) available: [details of any supplementary information available should be included here]. See DOI: 10.1039/x0xx00000x



Scheme 1. Challenges for enantioselective control in ACT and the strategy envisioned in this work.

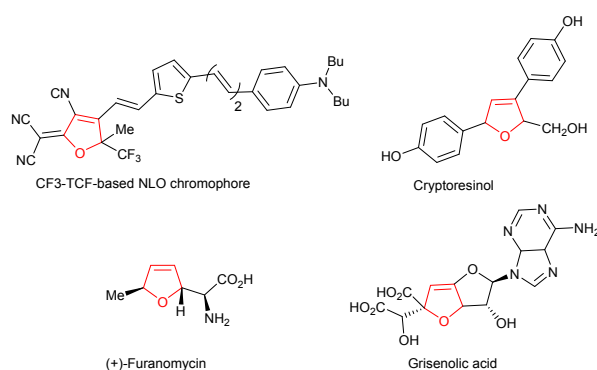


Figure 1. Molecules containing the 2,5-dihydrofuran motif.

drugs, core motifs in many natural products, and components of materials.²⁰ 2,5-Dihydrofuran containing molecules include the CF₃-TCF based nonlinear optical (NLO) chromophore,²¹ cryptoresinol,²² (+)-furanomycin,²³ and grisenolic acid²⁴ (Figure 1). These compounds possess intriguing properties such as electro-optical, antifungal, antibiotic, and anticancer activities. Given the therapeutic potential of 2,5-dihydrofurans, understanding the relationship between biological activity and stereochemistry is of interest. However, facile asymmetric syntheses of 2,5-dihydrofurans are not well developed.²⁵ Enantioselective construction of quaternary stereocenters in 2,5-dihydrofurans is quite challenging,²⁶⁻²⁸ with few documented examples.²⁹ Therefore, a new methodology for the catalytic, enantioselective synthesis of this important class of compounds would open new lines of pharmacological investigation. Herein, we report an enantioselective synthesis of 2,5-dihydrofurans with a quaternary center via Ag(I)-catalyzed formal [4+1] cycloaddition of diazoacetates and propargyl alcohols.

Results and discussion

In an attempt to directly adapt our Pd(II)-catalyzed reaction, we tested traditional chiral ligands of palladium catalysts, such as oxazolines, diimines, or BINAP, but these attempts resulted in minimal enantioselectivity (for details of substrate preparation and condition screening see supporting Information, Schemes S1-S3, and Table S1). Therefore, we decided to try other transition metal catalysts. Cu(OTf)₂, Cu(CH₃CN)₂PF₆, AgOTf, and AgSbF₆ are all known to catalyze this reaction.¹⁸ We used Zhou's chiral spiro-based diphosphine, **L1**,³⁰ as a standard ligand to test each of these catalysts and found AgSbF₆ afforded 2,5-dihydrofuran **3a** with 15% *ee*, while the other catalysts had minimal catalytic activities (Table 1, entries 1-4).

After discovering a functional catalyst, we turned our attention to enhancing the enantioselectivity through optimization of the chiral ligand. We explored oxazolines, diamines, amino alcohols, and diphosphines. Oxazolines **L2**, **L3**, **L4**,^{31, 32} diamines **L5**, **L6**,^{33, 34} and amino alcohol **L7**³⁵ afforded [1,2]-proton shift or [2,3]-sigmatropic rearrangement as the major products and showed no enantiomeric enrichment (Table 1, entries 5-10). However, BINAP **L8** gave **3a** as the major product with 54% *ee*. Further screening with other chiral phosphorous ligands including substituted BINAP derivatives **L9**, **L10**, **L11**, spirophosphines **L12** and fluorophos **L14**, indicated 3,5-DM-BINAP **L10** was the optimal ligand, giving **3a** as the major product with 76% *ee* (Table 1, entries 11-16). The enantioselectivity could be further improved to 78% by performing the reaction in the dark (Table 1, entry 17). The synergistic catalysis of the bifunctional Ag-complex, in combination with the proper BINAP-derived ligand, is likely to contribute to the observed chemo- and enantioselectivity.³⁶⁻³⁸

ARTICLE

Table 1. Catalyst and chiral ligand screening for formal [4+1] cycloaddition of diazoacetates and propargyl alcohols

Reaction scheme showing the formal [4+1] cycloaddition of diazoacetate **1a** and propargyl alcohol **2a** to form products **3a**, **4a**, **5a**, and **6a**. Conditions: Chiral catalyst (10 mol%), DCM, 4Å MS, 25°C.

Chemical structures of ligands L1 through L13 are shown below the reaction scheme. L1-L7 are various phosphine and nitrogen-containing ligands. L8-L13 are ferrocenyl phosphine ligands with different substituents (Ar).

Legend for L8-L13:
L8 Ar= phenyl
L9 Ar= 4-methylphenyl
L10 Ar= 3,5-dimethylphenyl
L11 Ar= 3,5-dimethyl-*t*-butylphenyl

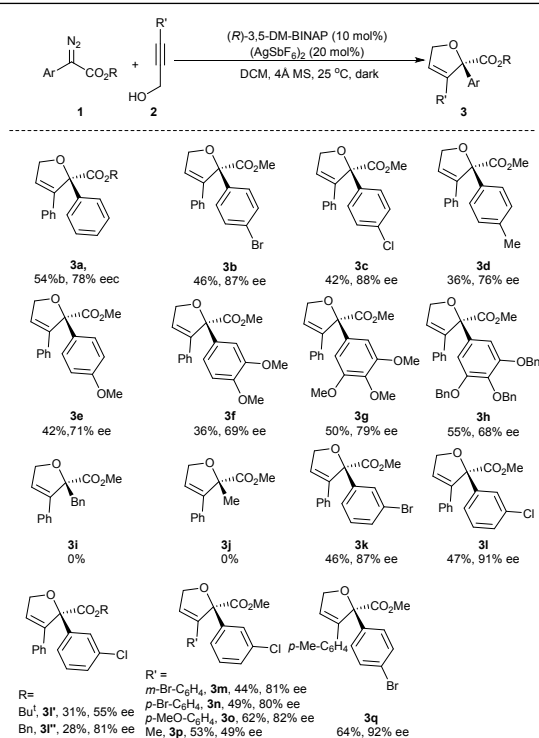
Entry	M	L	M:L	con. ^b (%)	3a:4a:5a:6a^b	ee ^c (%)
1	Cu(OTf) ₂	L1	1:1	<5	-	-
2	Cu(CH ₃ CN) ₄ PF ₆	L1	2:1	<5	-	-
3	AgOTf	L1	2:1	30	40:28:22:10	10
4	AgSbF ₆	L1	2:1	>90	44:24:21:11	15
5	AgSbF ₆	L2	1:1	>90	17:44:17:12	0
6	AgSbF ₆	L3	1:1	>90	25:42:23:10	0
7	AgSbF ₆	L4	1:1	>90	30:12:47:11	0
8	AgSbF ₆	L5	1:1	45	32:52:12:4	0
9	AgSbF ₆	L6	1:1	65	22:34:34:10	0
10	AgSbF ₆	L7	2:1	68	25:45:14:15	0
11	AgSbF ₆	L8	2:1	>90	57:12:16:15	54
12	AgSbF ₆	L9	2:1	>90	62:13:13:12	60
13	AgSbF ₆	L10	2:1	>90	65:10:15:10	76
14	AgSbF ₆	L11	2:1	68	49:21:18:12	53
15	AgSbF ₆	L12	2:1	>90	46:22:21:11	32
16	AgSbF ₆	L13	2:1	>90	37:23:24:16	20
17 ^d	AgSbF ₆	L10	2:1	>90	68:12:10:10	78

ARTICLE

^aReaction conditions: **1a** (0.15 mmol) in DCM (1.0 mL) was added to a solution of **2a** (0.15 mmol, 1.0 equiv), 150 mg 4Å MS, M (0.01 mmol, 0.1 equiv) and L (0.01 or 0.005 mmol, 0.1 or 0.05 equiv) in 1.0 mL of DCM, at 25°C. ^bDetermined by ¹H NMR of the reaction mixture. ^cDetermined by chiral HPLC analysis. ^dReaction was performed in the dark.

We next investigated the substrate scope of the Ag(I)-catalyzed asymmetric formal [4+1] cycloaddition of diazoacetates **1** and propargyl alcohols **2** (Table 2 and Scheme S4). Aryldiazoesters with halo substituents on the aromatic ring increased the enantioselectivity (Table 2, **3b-c**), while ones with electron-donating substituents on the aromatic ring showed similar enantioselectivities as those obtained in the case of the phenyldiazoester (Table 2, **3d-h**). Alkyldiazoacetates such as ethyl methyl diazoacetate and ethyl benzyl diazoacetate were tested as well, resulting in dimers of alkyldiazoacetates as the major product (Table 2, **3i-j**). The *meta*-halo diazo substrates also gave higher enantioselectivity than phenyldiazoester (Table 2, **3k-l**). The enhancement of enantiocontrol of halogen-bearing substrates was possibly due to the weak interactions between halogen and Ag catalyst. The yields and enantioselectivities dropped sharply in the cases of *tert*-butyl *meta*-chlorophenyldiazoacetate and benzyl *meta*-chlorophenyldiazoacetate, indicating the size of the ester group has a direct effect on the reactivity and enantioselectivity of the reaction (Table 2, **3l'** and **3l''**).

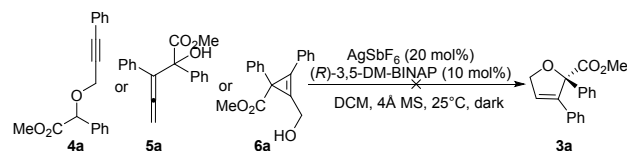
Table 2. Initial substrate scope of the Ag-catalyzed [4+1] cycloaddition reaction.^a



^aReaction conditions: **1** (0.2 mmol) in DCM (4 mL) was added to a solution of **2** (0.4 mmol, 2.0 equiv), 200 mg 4Å MS, AgBf₆ (0.04 mmol, 0.2 equiv) and (*R*)-3,5-DM-BINAP (0.02 mmol, 0.1equiv) in 2.0 mL of DCM at 25°C in the dark. ^bIsolated yield. ^cDetermined by chiral HPLC analysis.

Then, methyl *meta*-chlorophenyldiazoacetate was used as a standard substrate to explore the scope of aryl propargyl alcohols. By testing the effect of halo groups and methoxy on the aromatic ring of propargyl alcohols (Table 2, **3m-o**), all substitutions gave high *ees* (80–82%). But the methoxy group was better than the bromo group in terms of yield. Notably, 3-methyl propargyl alcohol was compatible in the reaction with 53% yield and 49% *ee* (Table 2, **3p**). Interestingly, the combination of *para*-bromophenyldiazoacetate and *para*-methylphenylpropargyl alcohol could generate **3q** in 62% yield and 92% *ee*. Overall, with these initial conditions, the reaction could produce 2,5-dihydrofurans with moderate yields and good to excellent enantioselectivities.

In an effort to improve the yield and stereoselectivity of the Ag(I)-catalyzed [4+1] cycloaddition, we sought to understand the reaction mechanism. Although we postulated this reaction proceeded via a formal cycloaddition, we could not rule out another pathway. It was reasoned that the formation of **3a** may proceed through one of the other three reaction products: the [1,2]-proton shift product **4a**, the [2,3]-sigmatropic rearrangement product **5a**, or cyclopropene **6a**. To test this possibility, we isolated each of these products and subjected them to the optimized conditions for the formation of **3a** (Scheme 2). In no case did we observe the formation of **3a**, ruling out **4a**, **5a**, or **6a** as intermediates, and offering support to our mechanistic hypothesis.



Scheme 2. Product **3a** does not derive from by-products **4a**, **5a** or **6a**.

We next sought to characterize the structure of the reactive catalytic species. The coordination model of AgOTf and BINAP is known to be related to the ratio of AgOTf and ligand and the counter-ion of the complex.³⁹ However, the coordination model of AgSbF₆ and (*R*)-3,5-DM-BINAP has not been reported. To explore the structure of the active catalytic species, we titrated AgSbF₆ into (*R*)-3,5-DM-BINAP and measured the proton

nuclear magnetic resonance (^1H NMR) spectra. At a AgSbF_6 :(*R*)-3,5-DM-BINAP ratio of 2:1, the ^1H NMR spectra no longer changed (Supporting Information, Figure S1). In addition, we monitored ^{31}P NMR spectra while carrying out the same titration. Matching the ^1H NMR data, we observed disappearance of the sharp free phosphine peak at the same 2:1 ratio of catalyst to ligand (Supporting Information, Figure S2). High resolution mass spectrometry analysis of the 2:1 molar ratio complex of AgSbF_6 and (*R*)-3,5-DM-BINAP showed the predicted signal for $\{[(R)\text{-}3,5\text{-DM-BINAP}]\text{Ag}_2\}^{2+}$ (Supporting Information, Figure S3).

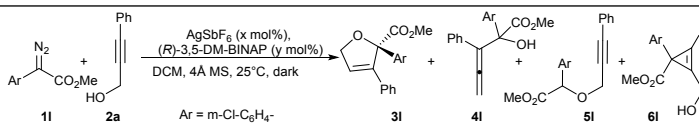
To confirm the functional significance of these data, we varied the ratio of ligand to catalyst and carried out the reaction. When the molar ratio of AgSbF_6 and (*R*)-3,5-DM-BINAP was lower than 2:1, both chemoselectivity and enantioselectivity decreased (Table 3, entries 1-5), while only reduction of the loading of the complex of AgSbF_6 and (*R*)-3,5-DM-BINAP without changing the 2:1 molar ratio did not influence enantioselectivity (Table 3, entry 1 vs entry 5). Taken together, these data indicate the reactive catalytic species of this formal [4+1] cycloaddition of diazoacetates and propargyl alcohols is $\{[(R)\text{-}3,5\text{-DM-}$

BINAP] $(\text{AgSbF}_6)_2$ (**9**), and not $\{[(R)\text{-}3,5\text{-DM-BINAP}]\text{AgSbF}_6\}$ (**8**) (Scheme 3).

DOI: 10.1039/C9OB01903K

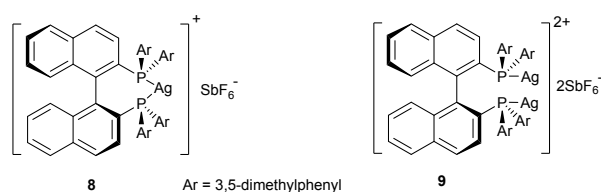
We next asked how many molecules of **9** are needed for each catalytic cycle. To answer this question, we performed the reaction using **9** with varied *ee* values, resulting in a positive nonlinear relationship between the *ee* values of product **3I** and **9** (Figure 2a and Scheme S5). The result implicates more than one molecule of **9** involved in the key transition state, since a positive nonlinear effect is usually caused by enantioselectivity enrichment during the formation of a multimeric active catalytic species or a synergistic catalytic system.⁴⁰⁻⁴⁵ When the combination of 5 mol% $\text{Rh}_2(\text{OAc})_4$ and 10 mol% **9** was used as catalyst, both chemoselectivity and enantioselectivity of **3I** were decreased (Scheme S6). This indicates that the formation of the Ag-carbenoid and the synergy between the two molecules of **9** is critical to the stereoselective cyclization step because the presence of $\text{Rh}_2(\text{OAc})_4$ likely generates the more reactive Rh-carbenoid and disrupts the synergy of the two molecules of **9**. Then we questioned whether two molecules of **9** functioned on one molecule of substrate

Table 3. The effect of loading and ratio of (*R*)-3,5-DM-BINAP and AgSbF_6 on chemo- and enantioselectivity.^a



Entry	x	y	con. ^a (%)	3I : 4I : 5I : 6I ^b	3I , <i>ee</i> ^c (%)
1	20	10	>90	47:33:9:11	91
2	16	10	>90	40:14:11:35	82
3	14	10	>90	30:10:10:50	85
4	10	10	>90	22:10:6:62	85
5	10	5	>90	47:25:6:22	91

^aReaction conditions: **1I** (0.1 mmol) in DCM (1 mL) was added to a solution of **2a** (0.1 mmol, 1.0 equiv), 100 mg 4Å MS, AgSbF_6 (0.001x mmol, 0.01x equiv) and (*R*)-3,5-DM-BINAP (0.001y mmol, 0.01y equiv) in 2.0 mL of DCM at 25°C in the dark. ^bDetermined by ^1H NMR of the reaction mixture. ^cDetermined by chiral HPLC analysis



Scheme 3. Possible structures of the reactive catalyst.

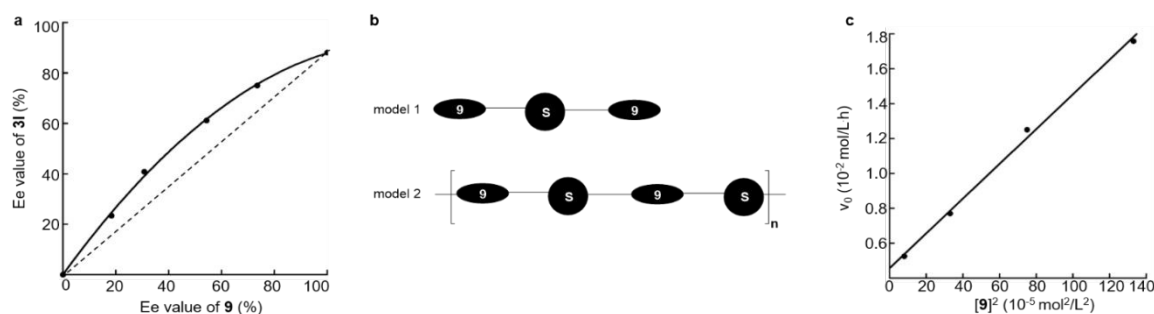


Figure 2. Mechanistic investigations. (a) Positive nonlinear effect of **9**. (b) Possible interaction models of substrate (**S**) and catalyst **9**. (c) Second order kinetics of **9**.

ARTICLE

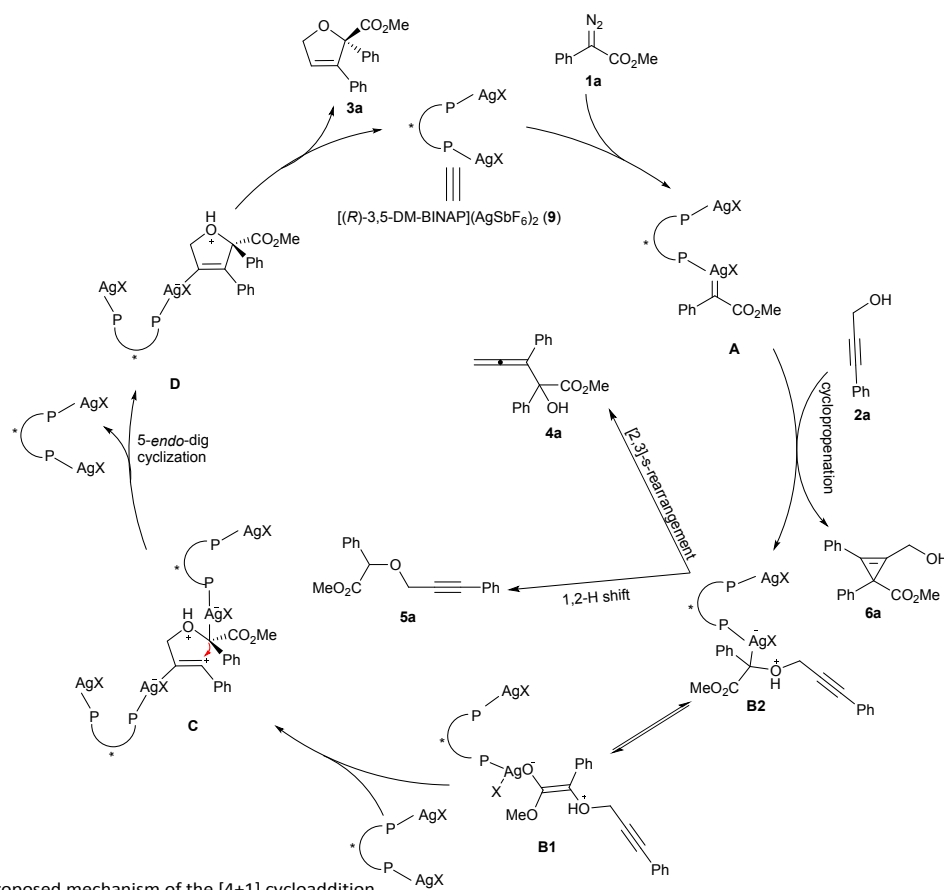
(Figure 2b, model 1) or **9** and its substrate form a polymeric chain with a 1:1 ratio (Figure 2b, model 2). To clarify this, the kinetic profile of **9** was investigated. A linear relationship between the initial reaction rates and the square of the catalyst concentration was revealed, representing second order kinetics of **9** (Figure 2c, Scheme S7, Figure S4, and Table S2). This indicated a second molecule of **9** must engage the substrate-**9** complex in the rate-limiting step, to generate one molecule of product **3l**. Hence, model 1 is likely to be the interaction fashion of catalyst **9** and its substrate.

Taking all of these data together, we propose the mechanism for the Ag(I)-catalyzed formal [4+1] cycloaddition of aryl diazoacetates and aryl propargyl alcohols shown in Scheme 4. Diazoacetate **1a** is decomposed by **9**, forming Ag-carbenoid **A**. The Ag-enolate **B1**, which is in equilibrium with Ag-associated oxonium ylide **B2**, is formed in situ from **A** and propargyl alcohol **2a**. **B1** or **B2** utilize another molecule of **9** in the alkyne coordinating site, thus generating a synergistic bi-catalyst species **C**, which undergoes a 5-*endo*-dig cyclization to form the final product **3a** through intermediate **D**. Side products **4a** and **5a** can be formed from **B1** or **B2** via a [2,3]-sigmatropic rearrangement and a [1,2]-proton shift, respectively.^{46, 47} Side product **6a** can be formed from **A** through cyclopropanation. Based on our mechanistic hypothesis, we reasoned we might further optimize the reaction by using a Brønsted base to

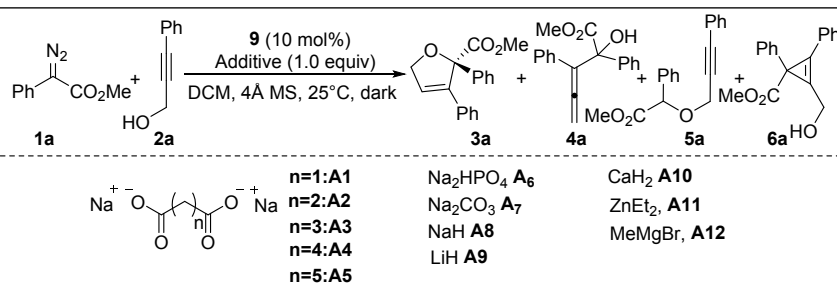
remove protons from the reaction, which might cut the side products **4a** and **5a** and stabilize the transition state. The Brønsted base must fulfill two requirements: 1) it must be basic enough to deprotonate propargyl alcohol to prevent the formation of side products; and 2) its coordination ability should not be strong enough to poison **9**. We also reasoned a di-base could potentially function as a linker between two molecules of **9**. With these requirements in mind, we screened a panel of Brønsted bases as additives (Table 4). First, a series of disodium carboxylates with varied linkers were evaluated. The reaction proceeded smoothly but with no improvement in chemo- or enantioselectivity (Table 4, entry 1-5). Second, a series of inorganic bases Na₂HPO₄, Na₂CO₃, NaH, and LiH were tested, resulting in no reaction due to the inhibition of **9** by their counter-ions that strongly coordinated the Ag. Finally, divalent metal bases including CaH₂, ZnEt₂, and MeMgBr were screened. CaH₂ improved chemoselectivity by suppressing generation of **5a** and slightly increased enantioselectivity from 78% to 81% (Table 4, entry 10). Both ZnEt₂ and MeMgBr poisoned **9** (Table 4, entry 11-12). The chemoselectivity was further improved if 2 equiv of **2a** or 2 equiv of both **2a** and CaH₂ were used (Table 4, entry 13-14). In short, by adding CaH₂, the chemoselectivity of this reaction could be increased by 17%.

Next, we used these new conditions and revisited the substrate scope. First, phenyl propargyl alcohol was set as the

ARTICLE



Scheme 4 Proposed mechanism of the [4+1] cycloaddition

Table 4. Additive screening for formal [4+1] cycloaddition of diazoacetates and propargyl alcohols.^a

Entry	Additives	con. ^b (%)	3a:4a:5a:6a ^b	ee ^c (%)
1	A1	>90	68:11:16:5	78
2	A2	>90	65:10:20:5	78
3	A3	>90	66:12:17:5	78

4	A4	>90	65:13:17:5	78 View Article Online DOI: 10.1039/C9OB01903K
5	A5	>90	63:12:20:5	78
6	A6	<5	-	-
7	A7	<5	-	-
8	A8	<5	-	-
9	A9	<5	-	-
10	A10	>90	75:10:10:5	81
11	A11	<5	-	-
12 ^d	A12	<5	-	-
13 ^e	A10	>90	80:5:10:5	81
14 ^{e,f}	A10	>90	85:5:5:5	81

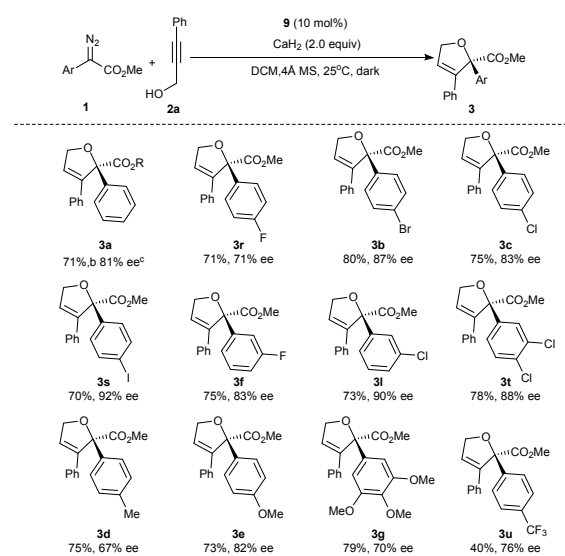
^aReaction conditions: **1a** (0.1 mmol) in DCM (1 mL) was added to a solution of **2a** (0.1 mmol, 1 equiv), 200 mg 4Å MS, AgSbF₆ (0.02 mmol, 0.2 equiv) and (*R*)-3,5-DM-BINAP (0.01 mmol, 0.1 equiv) in 2 mL of DCM at 25°C in the dark. ^bDetermined by crude ¹H NMR of the reaction mixture. ^cDetermined by chiral HPLC analysis. ^d1 equiv AgSbF₆ was added. ^e2 equiv **2a** was used. ^f2 equiv **A10** was used.

standard substrate to evaluate a panel of aryldiazoacetates (Table 5). With the new conditions, **3a** could be isolated in 71% yield (Table 5, **3a**) and 81% *ee*. Halogens, electron-donating groups (EDG), and electron-withdrawing groups (EWG) at the *para* position are all compatible with these reaction conditions, giving high yields (67-80%), with the exception of trifluoromethyl group, which gave only 40% yield, and 67-87% *ee*. (Table 5, **3b**, **3c**, **3d**, **3e**, **3r**, and **3s**). Notably, this is the first time EWG-containing diazoacetates show good reactivity in this cycloaddition reaction.^{18,19} The *m*-halo-substituted diazoacetates showed a significant increase in yield (73-75% yield vs 46-47% yield for the previous conditions) with no significant loss in enantio-induction (83-90% *ee*; Table 5, **3f** and **3l**). Diazoacetates with multiple chloro or methoxy substitutions were evaluated as well. Both afforded comparably high yields, but the 3,4-chloro-substituted diazoacetate had higher enantioselectivity than the 3,4,5-methoxy-substituted diazoacetate (Table 5, **3t** and **3g**).

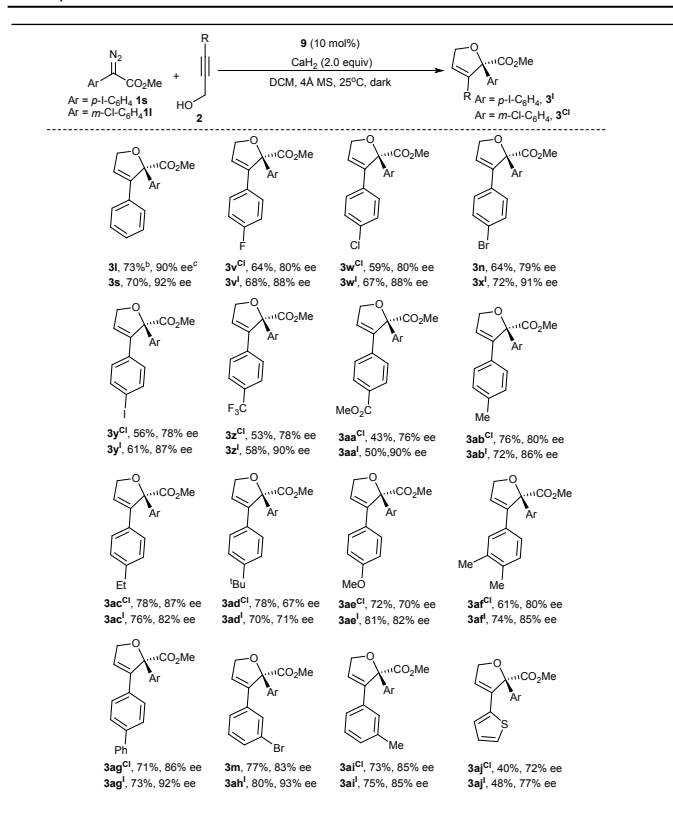
Then *p*-I and *m*-Cl substituted diazo, which had excellent enantio-induction were used as standard substrates to test a series of aryl propargyl alcohols. Generally, these two diazoacetates could offer comparable yields, but methyl *para*-iodophenyldiazoacetate gave higher *ee* except **3ac** and **3ai**. *p*-Br, *p*-CF₃, *p*-CO₂Me, *p*-Ph and *m*-Br substituted aryl propargyl alcohols showed excellent *ees* (Table 6, **3x**^{cl}, **3z**^{cl}, **3aa**^{cl}, **3ag**^{cl}, **3ah**^{cl}) with yields in the range of 58-80%. Their *m*-Cl counterparts had 76-86% *ees* and 43-77% yields (Table 6, **3x**^{cl}, **3z**^{cl}, **3aa**^{cl}, **3ag**^{cl}, **3m**). *p*-F, *p*-Cl, *p*-I, *p*-Me, *m*-Me, and 3,4-methyl-substituted propargyl alcohols gave 61-75% yields and 85-88% *ees* (Table 6, **3v**^{cl}, **3w**^{cl}, **3y**^{cl}, **3ab**^{cl}, **3ai**^{cl}, **3af**^{cl}). And their *m*-Cl analogues gave 59-76% yields and 78-85% *ees* (Table 6, **3v**^{cl}, **3w**^{cl}, **3y**^{cl}, **3ab**^{cl}, **3ai**^{cl}, **3af**^{cl}). *p*-Et, *p*-*tert*-Bu, and *p*-MeO substituted-phenyl propargyl alcohols generated 2,5-dihydrofurans with 71-82% yields and 70-82% *ees* (Table 6, **3ac**^{cl}, **3ad**^{cl}, **3ae**^{cl}), with their *m*-Cl parallels giving 72-78% yields and 67-87% *ees* (Table 6, **3ac**^{cl}, **3ad**^{cl}, **3ae**^{cl}). Interestingly, the heteroaromatic group, thiophene, is also compatible with the reaction, furnishing **3aj** with 40-80% yields and 72-77% *ees* (Table 6, **3aj**^{cl}, **3aj**^l). Generally speaking, with

CaH₂ as an additive, the reaction gave higher yields and *ees* and had much broader substrate scope for diazoacetates and propargyl alcohols. The result supports the hypothesis that a suitable Brønsted base additive could suppress the formation of side products and benefit enantioselectivities. We currently do not have a precise model for the effects of CaH₂ on the reaction.

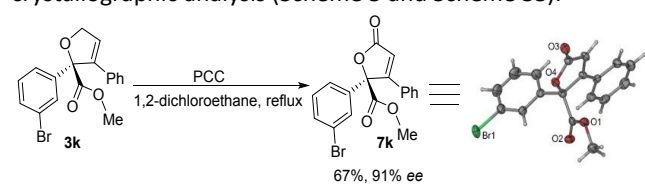
Table 5. Aryldiazoacetate scope of the Ag-catalyzed [4+1] cycloaddition reaction with optimized conditions.^a



^aReaction conditions: **1** (0.2 mmol) in DCM (2 mL) was added to a solution of **2a** (0.4 mmol, 2 equiv), CaH₂ (0.4 mmol, 2 equiv), 200 mg 4Å MS, AgSbF₆ (0.04 mmol, 0.2 equiv) and (*R*)-3,5-DM-BINAP (0.02 mmol, 0.1 equiv) in 2 mL of DCM at 25°C in the dark. ^bIsolated yield. ^cDetermined by chiral HPLC analysis.

Table 6. Aryl propargyl alcohol scope of the Ag-catalyzed [4+1] cycloaddition reaction with optimized conditions.^a

Finally, to unambiguously assign the absolute stereochemistry of the 2,5-dihydrofurans, the heavy atom-containing product **3k** was selected to transform into the corresponding lactone **7k** through PCC oxidation in 67% yield and 91% ee. The absolute configuration of **7k** was unambiguously confirmed as *S* by X-ray crystallographic analysis (Scheme 5 and Scheme S8).

**Scheme 5.** PCC-oxidation of **3k** and displacement ellipsoid plots (30% probability) of its product **7k**. (CCDC number: 1432486)

Conclusions

We have developed an asymmetric Ag(I)/(*R*)-3,5-DM-BINAP-catalyzed ACT method for the enantioselective synthesis of 2,5-dihydrofurans from aryl diazoacetates and propargyl alcohols. The synergistic catalysis of the bifunctional Ag(I)/(*R*)-3,5-DM-BINAP allows for high chemo- and enantioselectivities. Mechanistic investigations implied that the reaction involved two molecules of bifunctional catalyst **9** in the key transition state, which is the likely reason for the high chemoselectivities

and excellent enantioselectivities. Based on the mechanistic studies, basic additives were explored, and it was found that CaH₂ as an additive increased the chemo- and enantioselectivity. Synthetic application showed product **3k** could be readily transformed to lactone **7k**. The application of the synergistic catalysis of a bifunctional Ag catalyst in other ACT or Ag-nitrenoid transfer (ANT) is still ongoing in our lab.

Conflicts of interest

"There are no conflicts to declare".

Acknowledgements

We are grateful for the financial support from NSFC 21332003 (WH), the Program for Guangdong Introducing Innovative and Entrepreneurial Teams 2016ZT06Y337 (WH), the University of Arizona (EC), and the China Scholarship Council (TS). We also thank members of the Chapman and Hu labs for helpful discussions.

Notes and references

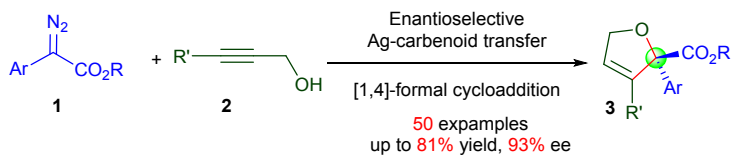
† Footnotes relating to the main text should appear here. These might include comments relevant to but not central to the matter under discussion, limited experimental and spectral data, and crystallographic data.

1. D. T. H. Phan and V. M. Dong, *Tetrahedron*, 2013, **69**, 5726-5731.
2. J. H. Hansen and H. M. L. Davies, *Chem. Sci.*, 2011, **2**, 457-461.
3. H. Pellissier, *Chem. Rev.*, 2016, **116**, 14868-14917.
4. F. Wang, P. Xu, F. Cong and P. P. Tang, *Chem. Sci.*, 2018, **9**, 8836-8841.
5. K. P. Wang, S. Y. Yun, P. Mamidipalli and D. Lee, *Chem. Sci.*, 2013, **4**, 3205-3211.
6. H. M. Wisniewska and E. R. Jarvo, *Chem. Sci.*, 2011, **2**, 807-810.
7. J. W. Park, B. Kang and V. M. Dong, *Angew. Chem. Int. Ed.*, 2018, **57**, 13598-13602.
8. N. Uhlig and C. J. Li, *Chem. Sci.*, 2011, **2**, 1241-1249.
9. G. C. Fang and X. H. Bi, *Chem. Soc. Rev.*, 2015, **44**, 8124-8173.
10. J. L. Ming, Q. Shi and T. Hayashi, *Chem. Sci.*, 2018, **9**, 7700-7704.
11. K. Juhl, R. G. Hazell and K. A. Jorgensen, *J. Chem. Soc. Per. Trans. 1*, 1999, 2293-2297.
12. S. Bachmann, D. Fielenbach and K. A. Jorgensen, *Organic & Biomolecular Chemistry*, 2004, **2**, 3044-3049.
13. J. F. Briones and H. M. L. Davies, *J. Am. Chem. Soc.*, 2012, **134**, 11916-11919.
14. H. Nakayama, S. Harada, M. Kono and T. Nemoto, *J. Am. Chem. Soc.*, 2017, **139**, 10188-10191.
15. G. L. Hamilton, E. J. Kang, M. Mba and F. D. Toste, *Science*, 2007, **317**, 496-499.

16. Y. Liang, H. L. Zhou and Z. X. Yu, *J. Am. Chem. Soc.*, 2009, **131**, 17783-17785.
17. T. D. Shi, X. Guo, S. H. Teng and W. H. Hu, *Chem. Comm.*, 2015, **51**, 15204-15207.
18. T. D. Shi, M. K. Wijeratne, C. Solano, A. J. Ambrose, A. B. Ross, C. Norwood, C. K. Orido, T. Grigoryan, J. Tillotson, M. Kang, G. Luo, B. M. Keegan, W. H. Hu, B. S. J. Blagg, D. D. Zhang, A. A. L. Gunatilaka and E. Chapman, *Biochemistry*, 2019, **58**, 3225-3231.
19. T. Shi, A. J. Ambrose, D. D. Zhang, W. Hu, and E. Chapman, manuscript in preparation.
20. R. Jacques, R. Pal, N. A. Parker, C. E. Sear, P. W. Smith, A. Ribaucourt and D. M. Hodgson, *Org. & Biomol. Chem.*, 2016, **14**, 5875-5893.
21. S. Liu, M. A. Haller, H. Ma, L. R. Dalton, S. H. Jang and A. K. Y. Jen, *Adv. Mater.*, 2003, **15**, 603-607.
22. K. Takahashi, M. Yasue and K. Ogiyama, *Phytochemistry*, 1988, **27**, 1550-1552.
23. M. M. Joullie, P. C. Wang and J. E. Semple, *J. Am. Chem. Soc.*, 1980, **102**, 887-889.
24. F. Nakagawa, T. Okazaki, A. Naito, Y. Iijima and M. Yamazaki, *J. Antibiot.*, 1985, **38**, 823-829.
25. X. P. Cheng, Z. X. Wang, C. D. Quintanilla and L. M. Zhang, *J. Am. Chem. Soc.*, 2019, **141**, 3787-3791.
26. J. W. Park, K. G. M. Kou, D. K. Kim and V. M. Dong, *Chem. Sci.*, 2015, **6**, 4479-4483.
27. Z. Q. Qian, F. Zhou, T. P. Du, B. L. Wang, M. Ding, X. L. Zhao and J. Zhou, *Chem. Comm.*, 2009, 6753-6755.
28. J. J. Murphy, D. Bastida, S. Paria, M. Fagnoni and P. Melchiorre, *Nature*, 2016, **532**, 218-222.
29. G. M. Borrajo-Calleja, V. Bizet, T. Burgi and C. Mazet, *Chem. Sci.*, 2015, **6**, 4807-4811.
30. J. H. Xie, L. X. Wang, Y. Fu, S. F. Zhu, B. M. Fan, H. F. Duan and Q. L. Zhou, *J. Am. Chem. Soc.*, 2003, **125**, 4404-4405.
31. G. Desimoni, G. Faita and K. A. Jorgensen, *Chem. Rev.*, 2006, **106**, 3561-3651.
32. F. Zhou, C. Tan, J. Tang, Y. Y. Zhang, W. M. Gao, H. H. Wu, Y. H. Yu and J. Zhou, *J. Am. Chem. Soc.*, 2013, **135**, 10994-10997.
33. H. Takahashi, T. Kawakita, M. Ohno, M. Yoshioka and S. Kobayashi, *Tetrahedron*, 1992, **48**, 5691-5700.
34. Y. Takemoto, *Org. & Biomol. Chem.*, 2005, **3**, 4299-4306.
35. E. J. Corey, R. K. Bakshi and S. Shibata, *J. Am. Chem. Soc.*, 1987, **109**, 5551-5553.
36. S. Liu, K. Chen, X. C. Lan, W. J. Hao, G. G. Li, S. J. Tu and B. Jiang, *Chem. Comm.*, 2017, **53**, 10692-10695.
37. A. E. Allen and D. W. C. MacMillan, *Chem. Sci.*, 2012, **3**, 633-658.
38. F. A. Cruz and V. M. Dong, *J. Am. Chem. Soc.*, 2017, **139**, 1029-1032.
39. N. Momiyama and H. Yamamoto, *J. Am. Chem. Soc.*, 2004, **126**, 5360-5361.
40. M. E. Noble-Teran, T. Buhse, J. M. Cruz, C. Coudret and J. C. Micheau, *Chemcatchem*, 2016, **8**, 1836-1845.
41. J. Inanaga, H. Furuno and T. Hayano, *Chem. Rev.*, 2002, **102**, 2211-2225.
42. N. Li, X. H. Chen, S. M. Zhou, S. W. Luo, J. Song, L. Ren and L. Z. Gong, *Angew. Chem. In. Ed.*, 2010, **49**, 6378-6381.
43. C. Girard and H. B. Kagan, *Angew. Chem. In. Ed.*, 1998, **37**, 2923-2959.
44. R. Noyori and M. Kitamura, *Angew. Chem. In. Ed.*, 1991, **30**, 49-69.
45. X. Tian, N. Hofmann and P. Melchiorre, *Angew. Chem. In. Ed.*, 2014, **53**, 2997-3000. DOI: 10.1039/C9OB01903K
46. Z. J. Li, V. Boyarskikh, J. H. Hansen, J. Autschbach, D. G. Musaev and H. M. L. Davies, *J. Am. Chem. Soc.*, 2012, **134**, 15497-15504.
47. J. F. Briones and H. M. L. Davies, *Org. Lett.*, 2011, **13**, 3984-3987.

Catalytic Asymmetric Synthesis of 2,5-Dihydrofurans Using Synergistic Bifunctional Ag Catalysis

Taoda Shi,^{a,b} Shenghan Teng,^a Alavala Gopi Krishna Reddy,^d Xin Guo,^c Yueteng Zhang,^b Kohlson T. Moore,^b Thomas Buckley,^b Damian J. Mason,^b Wei Wang,^b Eli Chapman,^{b*} and Wenhao Hu^{d*}



- ✓ Synergistic catalysis of a bifunctional Ag catalyst
- ✓ Mechanistic study on the reaction and catalyst
- ✓ Mechanism-guided discovery of CaH₂ as an additive
- ✓ High chemo- and enantioselectivities and broad substrate scope